Journal of Alloys and Compounds 511 (2012) 226–231

Contents lists available at SciVerse ScienceDirect

Journal of Alloys and Compounds

journal homepage: www.elsevier.com/locate/jallcom

Fabrication of A356 composite reinforced with micro and nano Al_2O_3 particles by a developed compocasting method and study of its properties

S.A. Sajjadi[a,*], M. Torabi Parizi[b], H.R. Ezatpour[a], A. Sedghi[c]

[a] Department of Materials Science and Metallurgical Engineering, Engineering Faculty, Ferdowsi University of Mashhad, Mashhad, Iran
[b] Department of Materials Science and Engineering, Saveh Branch, Islamic Azad University, Saveh, Iran
[c] Department of Materials Science and Metallurgical Engineering, Engineering Faculty, Imam Khomeini International University of Qazvin, Qazvin, Iran

ARTICLE INFO

Article history:
Received 15 March 2011
Received in revised form 9 August 2011
Accepted 9 August 2011
Available online 19 September 2011

Keywords:
Compocasting process
A356/Al_2O_3 composite
Microstructure

ABSTRACT

Aluminum/alumina composites are used in automotive and aerospace industries due to their low density and good mechanical strength. In this study, compocasting was used to fabricate aluminum–matrix composite reinforced with micro and nano-alumina particles. Different weight fractions of micro (3, 5 and 7.5 wt.%) and nano (1, 2, 3 and 4 wt.%) alumina particles were injected by argon gas into the semi-solid state A356 aluminum alloy and stirred by a mechanical stirrer with different speeds of 200, 300 and 450 rpm. The microstructure of the composite samples was investigated by Optical and Scanning Electron Microscopy. Also, density and hardness variation of micro and nano composites were measured. The microstructure study results revealed that application of compocasting process led to a transformation of a dendritic to a nondendritic structure of the matrix alloy. The SEM micrographs revealed that Al_2O_3 nano particles were surrounded by silicon eutectic and inclined to move toward inter-dendritic regions. They were dispersed uniformly in the matrix when 1, 2 and 3 wt.% nano Al_2O_3 or 3 and 5 wt.% micro Al_2O_3 was added, while, further increase in Al_2O_3 (4 wt.% nano Al_2O_3 and 7.5 wt.% micro Al_2O_3) led to agglomeration. The density measurements showed that the amount of porosity in the composites increased with increasing weight fraction and speed of stirring and decreasing particle size. The hardness results indicated that the hardness of the composites increased with decreasing size and increasing weight fraction of particles.

1. Introduction

Metal–matrix composites (MMCs) as new generation of materials can be used in many industries. In this group of materials a strong ceramic reinforcement is incorporated into a metal matrix to improve its properties including specific strength, specific stiffness, wear resistance, excellent corrosion resistance and high elastic modulus [1,2]. In other words, MMCs combine metallic properties of matrix alloys (ductility and toughness) with ceramic properties of reinforcements (high strength and high modulus) and lead to higher strength in tension and compression and higher service-temperature capabilities. Thus, they have significant scientific, technological and commercial importance [3].

Commonly micro-sized particles are used to improve yield and ultimate strength of alloys. However, ductility of MMCs decreases significantly with increasing ceramic particle concentration. On the other hand, application of nano-sized ceramic particles strengthens the metal–matrix composites while maintaining good ductility, high temperature creep resistance and better fatigue strength [4–6]. According to the literature however, it is revealed that addition of nano-alumina and copper simultaneously, improves microstructural characteristics and compressive response of AZ31B alloy [7].

MMCs are manufactured using different techniques. These techniques could be classified as liquid phase (casting) processes, vacuum infiltration, pressureless infiltration and dispersion methods. Liquid–solid processes are divided into compocasting and semi-solid forming. Solid-state processes or powder metallurgy (PM) techniques are extensively used in the manufacture of particle MMC [8,9]. Powder metallurgy routes are cost effective than the casting methods but cannot be used for the production of intricate shapes [8].

Compared with powder metallurgy, melt processing which involves stirring of ceramic particles into melt, has some important advantages: better matrix–particle bonding, easier control of matrix structure, simplicity, low cost of processing and nearer net shape and the wide selection of materials for this fabrication method [10,11]. Depending on the temperature at which the particles are introduced into the melt, there are two types of melting methods for making composites. In the liquid metallurgy

* Corresponding author. Fax: +98 511 8763305.
E-mail address: sajjadi@um.ac.ir (S.A. Sajjadi).

0925-8388/$ – see front matter © 2011 Elsevier B.V. All rights reserved.
doi:10.1016/j.jallcom.2011.08.105

process the particles are incorporated above the liquid temperature of the molten alloy, while in compocasting method the particles are incorporated into the semi-solid slurry temperature. It should be mentioned that there are two variations of the compocasting process namely semisolid–semisolid (SS) and semisolid–liquid (SL) process routes. They are distinguished from each other by the state of the matrix during the casting step, which is partially liquid or fully liquid for the SS and SL routes, respectively [12]. In both the processes, the vortex is used and the composites have high porosity. To decrease the porosity density in the composite material, the pressure casting such as die and squeeze casting methods are needed [12–14]. Squeeze casting has greater potential to create less defective cast components [15]. However, the melting process has two major problems: firstly, the ceramic particles are generally not wetted by the liquid metal matrix, and secondly, the particles tend to sink or float according to their density relative to the liquid metal. Consequently, the dispersion of the ceramic particles is not uniform, whereas powder metallurgy makes the uniform dispersion of the reinforcements [11,16,17]. However, in the melt method homogenization can be affected by manufacturing parameters such as: the crucible size, efficiency, size and shape of the impeller, temperature of the molten metal, stirring time and speed, particle feeding into the melt, and the temperature of the mold [11].

A356 aluminum alloy has been used as matrix of composites with ceramic reinforcing particles and fibers such as SiC and Al_2O_3 [18–20]. The alloy solidifies in a broad temperature interval (43 °C) and thus, is amenable to treatment in the semi-solid state as well as casting. Because of the wide temperature interval between the solidus and liquidus temperatures the alloy can be used as matrix for obtaining composites by compocasting method [21,22]. A356 aluminum alloy is a hypo eutectic Al–Si alloy and is promising candidate for automotive applications [23]. It is identified by good mechanical properties and high ductility, as well as excellent casting characteristics and high corrosion resistance. Mechanical properties of this alloy can be improved by appropriate heat treatment and especially using T6 heat treatment [3,24].

Although compocasting is generally accepted as a commercial route for the production of MMCs [13,14,25], there are technical challenges associated with producing a homogeneous, high density composite. The challenges rise up specially, with increasing alumina weight fraction and decreasing size of the particles, because of the poor wetting between matrix alloys and some reinforcements [26]. Most of the research works on fabrication of Al-based composites have concentrated on those containing micron-sized particles. The results of literature survey indicate that very low attempts have been made to investigate effects of the injection of particles by argon gas in compocasting method on the microstructure and mechanical properties of aluminum alloys reinforced with nano and micro-Al_2O_3 particles. So, the purpose of the present work is to produce reinforced metal–matrix composites with Al_2O_3 particles by compocasting method with injection of particles by argon gas and simultaneous use of impeller for both micro and nano sized particles. In addition, the effects of Al_2O_3 content, size, stirring speed and time on the distribution of Al_2O_3 particles into the metal–matrix and mechanical properties of the produced composites by quantitative analysis will be investigated.

2. Experimental procedures

In the present study, A356 aluminum alloy was used as the matrix material while the micro-Al_2O_3 (alumina) particles with particle size of 20–30 μm and nano Al_2O_3 particles with particle size of 50 nm (Merck Company) were used as reinforcements. Different sizes and weight fractions of the particles were used to investigate the influence of the parameters on the properties of the nano composites. The chemical composition of the A356 alloy was determined by optical emission spectroscopy (OES).

The composites were made by compocasting method using mechanical mixing of the molten matrix. At first step, 1000 g of Al-356 alloy was charged into the graphite crucible while an aperture was devised in the bottom for pouring of melt. The aperture was closed by a stopper during melting process and introduction of particles and opened for exiting of melt.

The alloy was melted in a laboratory electric resistive furnace by heating up to 680 °C. After melting, cleaning of the melt from the slag was performed by overheating of the melt 50 °C above the liquidus temperature. Mixing process was done by an impeller with a speed about 150 rpm at 610 °C in semi-solid condition. The impeller was designed to be able to make radial and axial forces in the melt. The mixing speed was then increased; the speed of 200, 300, and 450 rpm was investigated to determine the appropriate speed. To improve wettability, the ceramic particles were preheated at 300 °C before incorporation into the melt by argon gas. Before injection of particles, the mixing of semi-solid melt was carried out for 5 min to break the dendrites. Depending on the quantity of particles added, the injection time of the powder was 7–15 min. To study the effect of stirring time on distribution of reinforcement particles, after particle injection the slurry was stirred for 15 or 30 min. In the last stage, the slurry was heated to 650 °C and poured in a cylindrical sand mold. Specimens from longitudinal section were cut and prepared by mechanical polishing and then hardness tests were taken from samples (15 points with 1 cm interval in distance of 15 cm).

Characterization of the produced composite samples included metallographic examination, hardness measurement and density determination. For microstructure study, the specimens were prepared by grinding through 600, 800 and 1200 grit papers, respectively and then were polished with 6 μm diamond paste. The specimens were examined by Optical and Scanning Electron Microscopy (SEM).

The amount of porosity was determined by comparing the measured density from Archimedes method with their theoretical density. The hardness values (Brinell hardness) of the samples were measured on the polished samples in 3 points for each sample.

3. Results and discussion

3.1. Fabrication of composites

In the present work, A356 alloy was reinforced with micro and nano-sized Al_2O_3 particles. The chemical composition of A356 alloy is given in Table 1. The weight fractions of alumina in the composites were chosen as: 3, 5 and 7.5 wt.% for micro and 1, 2, 3 and 4 wt.% for nano, respectively. The composites have been successfully produced using compocasting method with injection of particles by argon gas.

3.2. Density and porosity

The experimental density of the composites was obtained by the Archimedian method of weighing small pieces cut from the composite cylinder first in air and then in water. In addition, the theoretical densities were calculated using the mixture rule [4,11]. The matrix alloy and Al_2O_3 particles have the densities of 2.7 and 3.9 g/cm^3, respectively [12]. In order to determine the porosity content, density measurements were conducted on unreinforced and composites reinforced with 3, 5 and 7.5 wt.% micro-Al_2O_3 and 1, 2, 3 and 4 wt.% nano-Al_2O_3 particles. The results are given in Table 2. The difference between the calculated density (D_c), which was obtained

Table 1
Chemical composition of A356 aluminum alloy.

Composition	Al	Si	Mn	Mg	Zn	Fe	Ti	Ni	P	Pb	Ca
wt.%	93.275	6.104	0.013	0.425	0.063	0.180	0.009	0.006	0.002	0.002	0.005

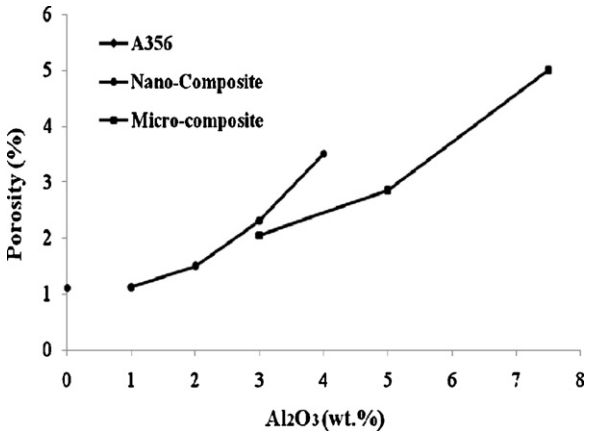

Fig. 1. The variation of porosity with nano and micro-Al_2O_3 particle content.

using chemical composition of the composites and the experimental density (D_e) is due to the existence of porosity in the structure.

The variation of porosity volume percent with nano and micro alumina volume percent is shown in Fig. 1. The figure shows that increasing porosity volume percent has occurred with increasing alumina weight fraction and decreasing particle size. This is due to the effect of low wettability and agglomeration at high content of reinforcement and pore nucleation at the matrix–Al_2O_3 interfaces. Moreover, decreasing liquid metal flow associated with the particle clusters leads to the formation of porosity. Such an observation has been reported in the literature [11,3,27]. Also, in a constant Al_2O_3 percent, the porosity percent of nano-composite was more than that of micro-composite because of the low wettability and more agglomeration and particle clustering of nano particles in comparison with micro particles.

Table 2
Calculated and experimental densities of unreinforced alloy and the composites.

Samples	Calculated density (D_c) (g/cm^3)	Experimental density (D_e) (g/cm^3)
A356	2.7	2.67
A356–3 wt.% Al_2O_3	2.736	2.679
A356–5 wt.% Al_2O_3	2.76	2.681
A356–7.5 wt.% Al_2O_3	2.81	2.669
A356–1 wt.% Al_2O_3	2.712	2.681
A356–2 wt.% Al_2O_3	2.724	2.683
A356–3 wt.% Al_2O_3	2.726	2.673
A356–4 wt.% Al_2O_3	2.752	2.665

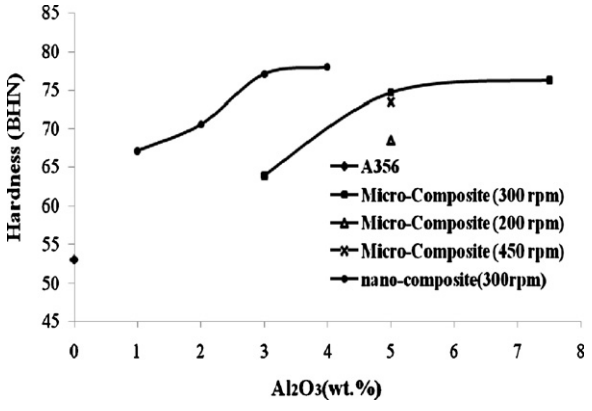

Fig. 2. Variation of hardness with nano and micro-Al_2O_3 particle content and stirring speed.

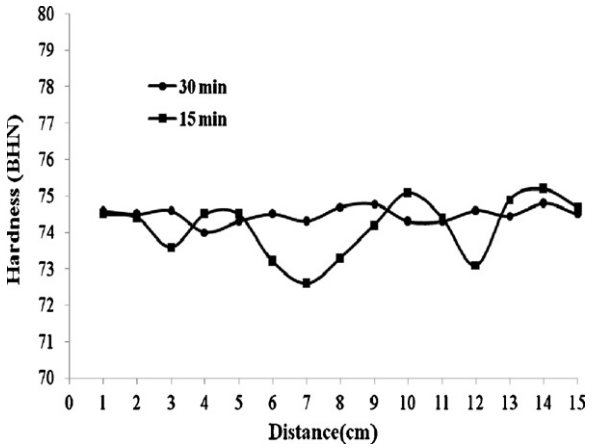

Fig. 3. Effect of stirring time on distribution of hardness (BHN) of composite with 5 wt.% micro-Al_2O_3 particles at 300 rpm stirring.

3.3. Hardness

The hardness tests were performed with a Brinell hardness machine using 10 kg load and a 2.5 mm diameter ball. For composite materials containing a soft matrix and a hard reinforcement phase, as in the case of alumina reinforced composites, the selection of a region in the sample for evaluating the hardness data is very crucial. Therefore, in order to obtain the average values of hardness, areas predominant in the soft matrix or in the hard phase should be avoided so that the average values of hardness are attained from these measurements.

3.3.1. Effect of weight fraction and size of reinforcement on hardness

The hardness results of the composites are shown in Fig. 2. Hardness of the composites increases with increasing particles weight fraction and with decreasing particles size. The higher hardness of the composite samples relative to that of the matrix–Al-alloy could be attributed to the reducing grain size and existence of Al_2O_3 hard particles acting as obstacles to the motion of dislocation. Also, the hardness of nano-composites was greater than that of micro-composites because of the more influence of nano particles on the strengthening mechanism (Orowan mechanism). With increasing alumina weight percent, scattering of hardness results increases because of non-uniform distribution of the reinforcement particles. It should be mentioned that agglomeration occurs as a result

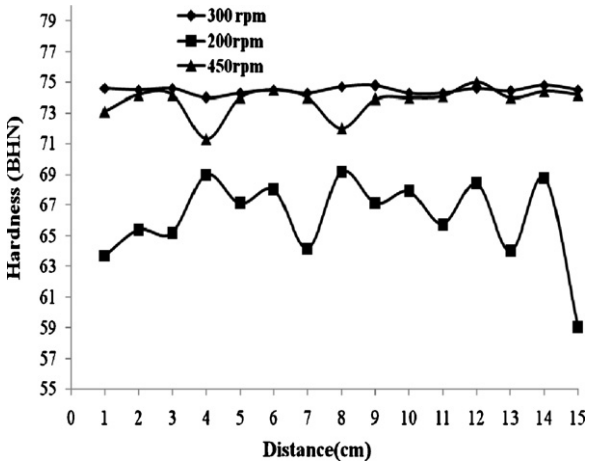

Fig. 4. Effect of stirring speed on distribution of hardness (BHN) of composite with 5 wt.% micro-Al_2O_3 particles at 30 min stirring.

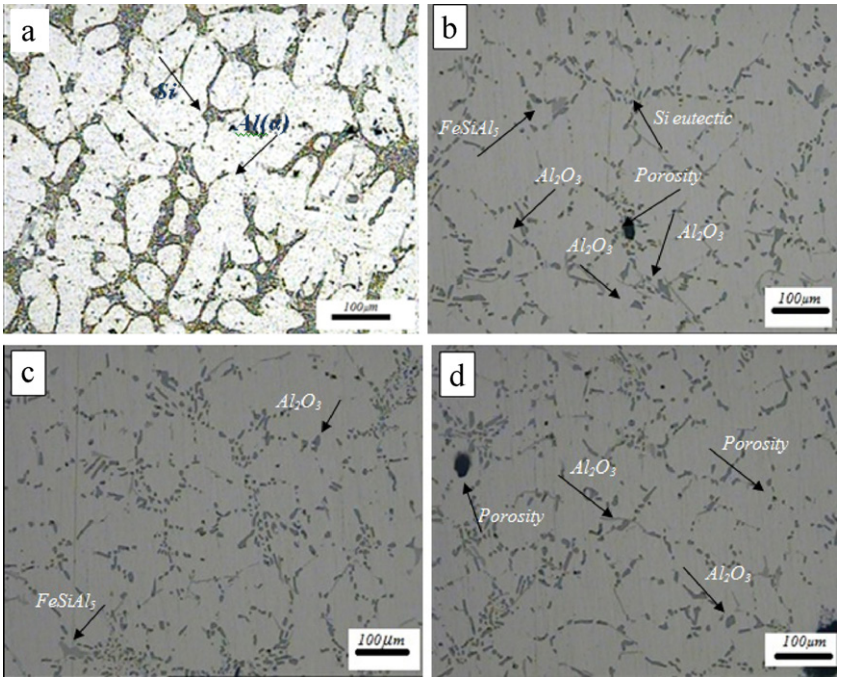

Fig. 5. Optical micrographs of micro-composites reinforced with 5 wt.% alumina and stirring speed of (a) 0, (b) 200, (c) 300 and (d) 450 rpm.

of higher viscosity and increasing tendency to clump the particles together due to high surface tension and poor wetting between the particles and the melt.

3.3.2. Effect of stirring time and speed on hardness

In the lower stirring time, particle clustering occurred so that in some places the matrix was identified without Al_2O_3 particles. Consequently, this caused remarkable changes in hardness value at the different locations in the specimen. By increasing the stirring time, better homogeneous distribution of Al_2O_3 in the Al matrix was found. The hardness results are reported in Fig. 3. It can be concluded from the figure that 30 min stirring shows uniform hardness distribution when compared to the lower stirring time.

Fig. 2 shows that hardness of the composite increases with increasing stirring speed up to 300 rpm because of homogeneous distribution of Al_2O_3 in the metal matrix and also, partly due to the decreasing grain size of the matrix. However when stirring speed increased too much (450 rpm), the particles were dispersed out of the crucible and so particle addition was not benefit. Due to the severe agitation of the melt surface and agglomeration of particles the hardness distribution is not uniform at 450 rpm (Fig. 4). In addition, according to Fig. 2, at lower stirring speed (200 rpm) the hardness values decreased because of agglomeration and imperfect incorporation of particles. In conclusion the hardness distribution is not uniform in this condition too (Fig. 4).

3.4. Microstructure

The as-cast microstructure of A356 alloys according to the equilibrium phase diagram consists of primary α phase (Al(α)) and a eutectic phase (Si) in the space between the particles (Fig. 5a). The results show that during solidification of A356–Al_2O_3 composite melt, Al_2O_3 particles are pushed by aluminum dendrites into the last freezing eutectic liquid. Therefore, Al_2O_3 particles are surrounded by silicon eutectic.

3.4.1. Effect of stirring speed and time on microstructure

The structure of the matrix alloy is dendritic but the shear forces produced by the rotation of the mixer cause a transformation of dendritic to non-dendritic structure of the primary α phase particles.

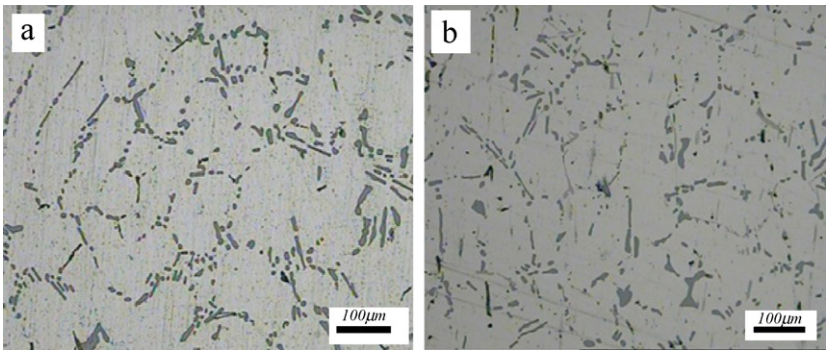

Fig. 6. Optical micrographs of micro-composites reinforced with (a) 3 and (b) 7.5 wt.% Al_2O_3, with stirring speed of 300 rpm.

The results of microstructure study reveal good interfacial bonding between aluminum matrix and Al_2O_3 particles and uniform dispersion of the particles throughout the matrix with low agglomeration. This can be attributed to the use of argon gas for injection and the good wettability of particles with melt in the semi-solid zone.

Fig. 5a–d shows that with increasing stirring speed homogeneous distribution of the particles has been achieved and the grain size decreases because of breaking of dendrites and enhancement of grain nucleation sites. Among the different stirring speeds investigated in this research, the optimum stirring speed was 300 rpm (Fig. 5c). At the higher stirring speed (450 rpm) due to the high turbulence and increasing of air bubbles and under the effect of centrifugal force, the particles were dispersed out of the crucible by the wind of the impeller and so particle addition was not achieved. Consequently, porosity formation and segregation at a macro level and inhomogeneous distribution of the strengthening particles occur (Fig. 5d). The lower stirring speed (200 rpm) causes decrease in wettability and increase in agglomeration of particles.

It is also understood from the microstructures that the increase in speed alone, will not distribute the particles; the stirring time is also another decisive factor. Higher stirring time and speed result in better distribution of particles (Fig. 3) but this can lead to the chemical reactions between matrix and particles, which often results in formation of brittle secondary phases [28,29].

3.4.2. *Effect of weight fraction and size of reinforcement on microstructure*

Figs. 5 and 6 show that addition of Al_2O_3 particles to A356 alloy affects the size of aluminum dendrites and eutectic morphology. The particles act as nucleation sites therefore eutectic size decreases. When 3 and 5 wt.% alumina are added to the melt (Figs. 5b and 6a) the particles are dispersed uniformly with low agglomeration at the matrix while the further addition (7.5 wt.% Al_2O_3) of particles causes the agglomeration of particles (Fig. 6b) and increase of porosity percent (Fig. 1) and less increase of harness (Fig. 2).

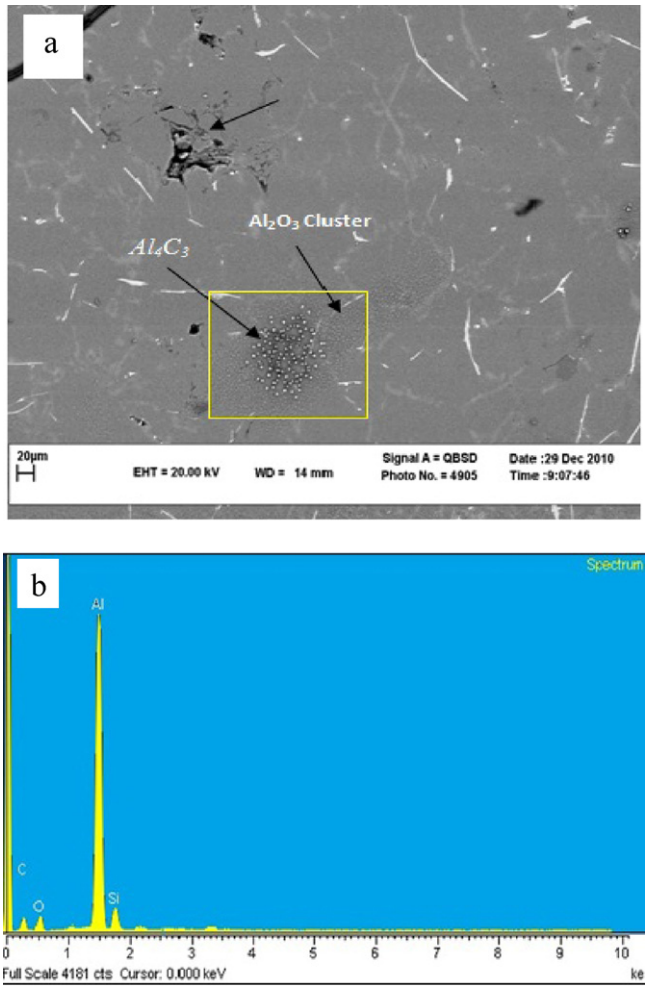

Fig. 7. (a) SEM and (b) EDS micrograph of nano-composites reinforced with 1 wt.% Al_2O_3.

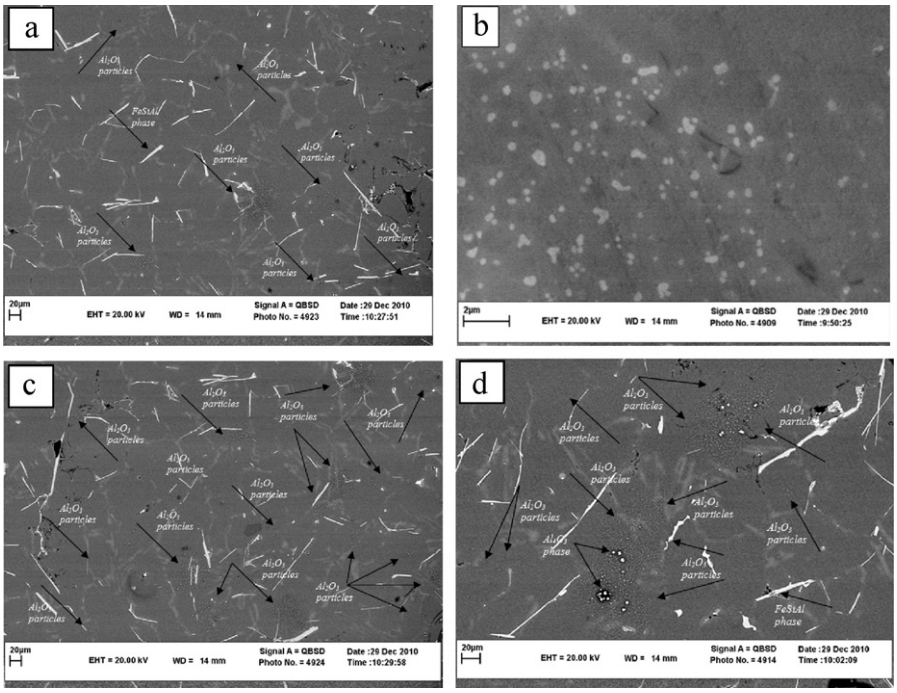

Fig. 8. SEM micrographs of nano-composites reinforced with: (a) 2 wt.% Al_2O_3; (b) 2 wt.% Al_2O_3 at higher magnification; (c) 3 wt.% Al_2O_3 and (d) 4 wt.% Al_2O_3, with stirring speed of 300 rpm.

The SEM micrograph and EDS result of nano-composite with 1 wt.% Al_2O_3 produced at stirring speed of 300 rpm are shown in Fig. 7. In the figure, the larger particles (brighter ones) are Al_4C_3 located next to the smaller particles which are nano-particles of Al_2O_3. Also, the duller blade-like Si crystals can be clearly observed. The bright plate-shape phases observed in the figure were recognized as the iron intermetallic phase of $FeSiAl_5$.

The SEM micrographs of nano-composites with 2, 3 and 4 wt.% Al_2O_3 are shown in Fig. 8. The SEM results indicate that the Al_2O_3 nano particles have tendency to segregate and cluster at inter-dendritic region and are surrounded by eutectic silicon. The micrographs reveal that in the case of 1, 2 and 3 wt.% Al_2O_3 (Fig. 8a–c) the nano particles disperse uniformly in the matrix with low agglomeration while, further increase in Al_2O_3 (4 wt.%) leads to more agglomeration (Fig. 8d). Because hardness of the specimen with 4 wt.% nano alumina does not improve considerably in comparison with the specimens with lower reinforcement particles it could be concluded that there is strong mechanical bonding between Al and Al_2O_3 particles in the specimens with low agglomeration.

4. Conclusions

In the current research micro and nano-composites of A356/Al_2O_3 were produced by compocasting method and with various conditions. The effects of different fabrication parameters on the microstructure and some physical and mechanical properties of the composites have been investigated. The following conclusions have been drawn:

a. The optimum conditions for fabrication of the composites were: preheating of the particles at 300 °C before injection, using of argon gas for injection particles, the injection time of 7–15 min according to the volume percent of particles, the stirring speed of 300 rpm and pouring temperature of 650 °C.
b. The amount of porosity increased with increasing the weight fraction and decreasing size of particles.
c. The hardness of the composites increased with increasing particle weight fraction and decreasing particles size. Also, the hardness distribution becomes more uniform with increasing stirring speed and time to an optimum level (300 rpm and 30 min).
d. The metallography study showed that the uniform dispersion of the micro-size particles was achieved in the composites reinforced with up to 5 wt.% micro-size particles while with 7.5 wt.% micro-size Al_2O_3 the agglomeration of particles occurred.
e. The SEM results showed that the Al_2O_3 nano particles inclined to segregate and cluster at inter-dendritic region and were surrounded by silicon eutectic.
f. The nano particles of Al_2O_3 were dispersed uniformly in the matrix when 1, 2 and 3 wt.% Al_2O_3 was added. Further increase in Al_2O_3 content (4 wt.%) led to the agglomeration.

Acknowledgements

The authors wish to express appreciation to the Ferdowsi University of Mashhad for supporting this project. Also, we acknowledge the careful assistance of Mr. H. Beygi and Mr. H. Sadeghi.

References

[1] G.S. Hanumanth, G.A. Irons, J. Mater. Sci. 28 (1993) 2459–2465.
[2] Y. Sahin, S. Murphy, J. Mater. Sci. 34 (1996) 5399–5407.
[3] A. Vencla, I. Bobicb, S. Arosteguic, B. Bobicd, A. Marinkovica, M. Babice, J. Alloys Compd. 506 (2010) 631–639.
[4] A. Mazaherya, H. Abdizadeha, H.R. Baharvandib, Mater. Sci. Eng. A 518 (2009) 61–64.
[5] B. Xionga, Z. Xu, Q. Yan, B. Lu, C. Cai, J. Alloys Compd. 509 (2011) 1187–1191.
[6] S.A. Sajjadi, H.R. Ezatpour, M. Torabi Parizi, J. Mater. Des. 34 (2012) 106–111.
[7] Q. Nguyen, M. Gupta, J. Alloys Compd. 490 (2010) 382–387.
[8] B.S. Ünlü, J. Mater. Des. 29 (2008) 2002–2008.
[9] S. Amirkhanlou, B. Niroumand, J. Mater. Des. 32 (2011) 1895–1902.
[10] M.A. Taha, N.A. El-Mahallawy, J. Mater. Process. Technol. 73 (1998) 139–146.
[11] M. Kok, J. Mater. Process. Technol. 161 (2005) 381–387.
[12] H. Sevik, S. Can Kurnaz, J. Mater. Des. 27 (2006) 676–683.
[13] S. Amirkhanlou, M.R. Rezaei, B. Niroumand, M.R. Toroghinejad, J. Mater. Des. 32 (2011) 2085–2090.
[14] B. Abbasipour, B. Niroumand, S.M. Monir Vaghefi, J. Trans. Nonferrous Met. China 20 (2010) 1561–1566.
[15] G.R. Li, Y.T. Zhao, H.M. Wang, G. Chen, Q.X. Dai, X.N. Cheng, J. Alloys Compd. 471 (2009) 530–535.
[16] R. Asthana, P.K. Rohatgi, Z. Metallk. 83 (12) (1992) 887–892.
[17] I.A. Ibrahim, F.A. Mohamed, E.J. Lavernia, J. Mater. Sci. 26 (1991) 1137–1156.
[18] P. Rohatgi, JOM 42 (1991) 10–15.
[19] H. Ribes, M. Suéry, Scripta Metall. 23 (1989) 705–709.
[20] A. Daoud, W. Reif, J. Mater. Process. Technol. 123 (2002) 313–318.
[21] X. Yang, Y. Jing, J. Liu, J. Mater. Process. Technol. 130–131 (2002) 569–573.
[22] M. Paes, E.J. Zoqui, Mater. Sci. Eng. A 406 (2005) 63–73.
[23] J.G. Conley, J. Huang, J. Asada, K. Akiba, Mater. Sci. Eng. A 285 (2000) 49–55.
[24] A. Kearney, E.L. Rooy, ASM Handbook, vol. 2, ASM International, Metals Park, 1990, pp. 123–151.
[25] J.T. Lin, D. Bhattacharyya, C. Lane, Wear 883 (1995) 181–183.
[26] S. Naher, D. Brabazon, L. Looney, J. Mater. Process. Technol. 143–144 (2003) 567–571.
[27] M. Kok, Ph.D. Thesis, Firat University, Elazıg, Turkey, 2000.
[28] S. Balasivanandha Prabu, L. Karunamoorthy, S. Kathiresan, B. Mohanb, J. Mater. Process. Technol. 171 (2006) 268–273.
[29] M. Singla1, D. Deepak Dwivedi, L. Singh, V. Chawla, J. Miner. Mater. Charact. Eng. 8 (2009) 455–467.